REFERENCES

Ahenach, J., Cool, P., and Vansant, E.F. (2000) Enhanced acidity created upon Al-grafting of porous clay Brönsted heterostructures *via* aluminium acetylacetonate adsorption, Phys. Chem. Chem. Phys., 2, 5750-5755.

Arau´jo, E.M., Me´lo, T.J.A., Santana, L.N.L., Neves, G.A., Ferreira, H.C.,Lira, H.L., Carvalho, L.H., A'vila Jr., M.M., Pontes, M.K.G., and Arau´jo, I.S. (2004) The influence of organo-bentonite clay on the processing and mechanical properties of nylon 6 and polystyrene composites. Materials Science and Engineering B, 112, 175–178.

Benjelloun, M., Cool, P., Linssen, T., and Vansant, E.F. (2001) Acidic porous clay heterostructures: study of their cation exchange capacity, Micropor. Mesopor. Mater., 49, 83-94.

Chen, L., Wong, S.C., and Pisharath, S. (2003) Fracture Properties of Nanoclay-Filled Polypropylene, J Appl Polym Sci, 88, 3298–3305.

Ding, C., Jia, D., He, H., Guo, B., and Hong, H. (2005) How organo-montmorillonite truly affects the structure and properties of polypropylene, Polymer Testing, 24, 94–100.

Fabio, B., Maurizio, C., Guido, A., Giovanna,C., and Luciano, F. (2006) Characterization and thermal degradation of polypropylene-montmorillonite nanocomposites, Polymer Degradation and Stability, 91, 600-605.

Galgali, G., Ramesh, C., and Lele, A. (2001) A Rheological Study on the Kinetics of Hybrid Formation in Polypropylene Nanocomposites, Macromolecules, 34, 852-858.

Galarneau, A., Barodawalla, A., and Pinnavaia, T.J. (1995) Porous Clay Heterostructures Formed by Gallery-Templated Synthesis, Nature, 374, 529-531.

Gilman, J.W. (1999) Flammability and thermal stability studies of polymer layered-silicate (clay) nanocomposites, Applied Clay Science, 15, 31–49.

Gregg, S.J., and Sing, K.S.W., Adsorption, Surface Area and Porosity, second ed., edition, Academic Press, London, 1982, pp. 4 and 116.

Kawasumi, M., Hasegawa, N., Kato, M., Usuki, A., and Okada, A. (1997) Preparation and Mechanical Properties of Polypropylene-Clay Hybrids, Macromolecules, 30, 6333-6338.

Lange, J., and Wyser, Y. (2003) Recent Innovations in Barrier Technologies for Plastic Packaging – a Review, Packaging Technology and Science, 16, 149-158.

LeBaron, P.C., Wang, Z., and Pinnavaia, T.J. (1999) Polymer-Layered Silicate Nanocomposites : an Overview, Applied Clay Science, 15, 11-29.

Manias, E., Touny, A., Wu, L., Strawhecker, K., Lu, B., and Chung, T.C. (2001) Polypropylene/Montmorillonite Nanocomposites. Review of the Synthetic Routes and Materials Properties, Chem. Mater., 13, 3516-3523.

Mercier, L., and Pinnavaia, T.J. (1998) A Functionalized Porous Clay Heterostructure for Heavy Metal ion (Hg^{2+}) trapping, Micropor. Mesopor. Mater., 20, 101-106.

Morlat, S., Mailhot, B., Gonzalez, D., and Gardette, J.L. (2004) Photo-oxidation of Polypropylene/Montmorillonite Nanocomposites. 1. Influence of Nanoclay and Compatibilizing Agent. Chem. Mater., 16, 377-383.

Nakatsuji, M., Ishii, R., Wang, Z.M., and Ooi, K. (2004) Preparation of porous clay minerals with organic–inorganic hybrid pillars using solvent-extraction route, Journal of Colloid and Interface Science, 272, 158–166.

Perrin-Sarazin, F., and Ton-That, M.T., Bureau, M.N., and Denault, J. (2005) Micro- and Nano-structure in Polypropylene/Clay Nanocomposites, Polymer, 46, 11624-11634.

Pires, J., Araujo, A.C., Carvalho, A.P., Pinto, M.L., Gonzalez-Calbet, J.M., and Ramirez-Castellanos, J. (2004) Porous materials from clays by the gallery template approach: synthesis, characterization and adsorption properties, Micropor. Mesopor. Mater., 73, 175-180.

Polverejan, M., Pauly, T.R., and Pinnavaia, T.J. (2000) Acidic Porous Clay Heterostructures (PCH): Intragallery Assembly of Mesoporous Silica in Synthetic Saponite Clays, Chem. Mater., 12, 2698-2704.

Polverejan, M., Liu, Y., and Pinnavaia, T.J. (2002) Aluminated Derivatives of Porous Clay Heterostructures (PCH) Assembled from Synthetic Saponite

Clay: Properties as Supermicroporous to Small Mesoporous Acid Catalysts, Chem. Mater., 14, 2283-2288.

Ramos Filho, F.G., Melo, T.A., Rabello, M.S., and Silva, S.M. (2005) Thermal Stability of Nanocomposites Based on Polypropylene and Bentonite, Polymer Degradation and Stability, 89, 383-392.

Sinha Ray, S., and Okamoto, M. (2003) Polymer/layered silicate nanocomposites: a review from preparation to processing, Prog. Polym. Sci., 28, 1539-1641.

Stein, A., Melde, B.J., and Schroden, R.C. (2000) Hybrid Inorganic-Organic Mesoporous Silicates-Nanoscopic Reactors Coming of Age, Adv. Mater., 12, 1403-1419.

Tidjania, A., Wald, O., Pohl, M.M., Hentschel, M.P., and Schartel, B. (2003) Polypropylene–graft–maleic anhydride-nanocomposites: I-Characterization and thermal stability of nanocomposites produced under nitrogen and in air, Polymer Degradation and Stability, 82, 133–140.

Ton-That, M.T., Perrin-Sarazin, F., Cole, K.C., Bureau, M.N., and Denault, J. (2004) Polyolefin Nanocomposites: Formation and Development, Polymer Engineering and Science, 44, 1212-1219.

Wang, Y., Easteal, A.J., and Dong Chen, X. (1998) Ethylene and Oxygen Permeability Through Polyethylene Packaging Films, Packaging Technology and Science, 11, 169-178.

Wei, L., Tang, Y., and Huang, B. (2004) Novel acidic porous clay heterostructure with highly ordered organic–inorganic hybrid structure: one-pot synthesis of mesoporous organosilica in the galleries of clay, Microporous and Mesoporous Materials., 67, 175–179.

Zhou, C., Li, X., Ge, Z., Li, Q., and Tong, D. (2004) Synthesis and acid catalysis of nanoporous silica/alumina-clay composites, Catalysis Today, 93-95, 607-613.

Zhu, H.Y., Ding, Z., Lu, C.Q., and Lu, G.Q. (2002) Molecular engineered porous clays using surfactants, Applied Clay Science, 20, 165-175.

APPENDICES

Appendix A Calculations and Experimental Data

Gas Permeability

Gas permeation experiments were obtained from Brugger Gas Permeability Tester. The sample films were cut into circular shape with 110 mm in diameter according to ASTM 1434-82. The thickness of the films was measured with the peacock digital thickness gauge model PDN 12N by reading ten points at random position over the entire test area and the results were averaged. The films were placed in a desicator over $CaCl_2$ and kept for not less than 48 h. prior to test.

Gas trasmission rate (GTR)

$$GTR = \frac{\Delta M}{A \cdot \Delta t \cdot \Delta p}$$

Permeability (Q)

$$Q = \frac{\Delta M \cdot L}{A \cdot \Delta t \cdot \Delta p}$$

$$\therefore Q = GTR \times L$$

where:

$\frac{\Delta M}{\Delta t}$ = amount of gas passing through film in unit time (cm^3/s)

A = area (m^2)

Δp = the differntial partial pressure of the permeat gas across the film (bar)

L = film thickness (mm)

The gas permeability rate, G, in units of $cm^3/(m^2.day.bar)$ is calculated from,

$$G = \frac{7.76\times10^7 \times V}{78.5K \times 29N}$$

where:

V = volume of the evacuation chamber

K = absolute temperature (degrees Kelvin)

N = the slope of the graph which is determined by dividing the time (s) by the scale divisions (mm)

if the evacuation chamber volume, V, is 0.4370 cm^3 then this expression simplifies to,

$$G = \frac{1.49\times10^7}{KN} \quad cm^3/(m^2 \cdot day \cdot bar)$$

$$G = \frac{1.49\times10^7 \times 0.9896}{KN} \quad cm^3/(m^2 \cdot day \cdot atm)$$

Table A1 Time and scale divisions of PP at 299.7 K (Film thickness : 0.0968 mm)

Time (s)	Scale divisions (mm)
0	100
1800	83.5
2400	78
3000	72
3600	66.5

Slope (N) : 107.32

R^2 : 0.9998

Table A2 Time and scale divisions of PP-g-MA/PP at 297.7 K (Film thickness : 0.1211 mm)

Time (s)	Scale divisions (mm)
0	100.5
600	95
1380	87.5
1980	82
2580	75.5

Slope (N) : 103.78

R^2 : 0.9992

Table A3 Time and scale divisions of PMH-C_{12}/PP-g-MA/PP at 299.4 K (Film thickness : 0.1029 mm)

Time (s)	Scale divisions (mm)
0	100
660	93.5
1260	86.5
1860	80.5
2460	74

Slope (N) : 92.683

R^2 : 0.9996

Table A4 Time and scale divisions of PMH-C_{16}/PP-g-MA/PP at 298 K (Film thickness : 0.1235 mm)

Time (s)	Scale divisions (mm)
0	100
600	94
3120	70
3780	62.5
4380	58

Slope (N) : 102.62

R^2 : 0.9993

Table A5 Time and scale divisions of PMH-C_{18}/PP-g-MA/PP at 298.2 K (Film thickness : 0.1095 mm)

Time (s)	Scale divisions (mm)
0	100
600	93.5
1200	87
1800	80.5
2400	74

Slope (N) : 92.308

R^2 : 1

Table A6 Time and scale divisions of PBH-C_{12}/PP-g-MA/PP at 299.4 K (Film thickness : 0.0944 mm)

Time (s)	Scale divisions (mm)
0	100
600	93.5
1200	88
1800	81
2400	74.5

Slope (N) : 94.377

R^2 : 0.9988

Table A7 Time and scale divisions of PBH-C_{16}/PP-g-MA/PP at 298.1 K (Film thickness : 0.1233 mm)

Time (s)	Scale divisions (mm)
0	100
780	92
1380	85.5
1980	79
2580	72

Slope (N) : 92.227

R^2 : 0.9994

Table A8 Time and scale divisions of PBH-C_{18}/PP-g-MA/PP at 300K (Film thickness : 0.1201 mm)

Time (s)	Scale divisions (mm)
0	100
600	94
1200	87
1800	80.5
2520	73

Slope (N) : 92.433

R^2 : 0.9995

Appendix B Types of Adsorption Isotherm and Hysteresis Loop

Figure B1 Types of adsorption isotherm according to BDDT classification.

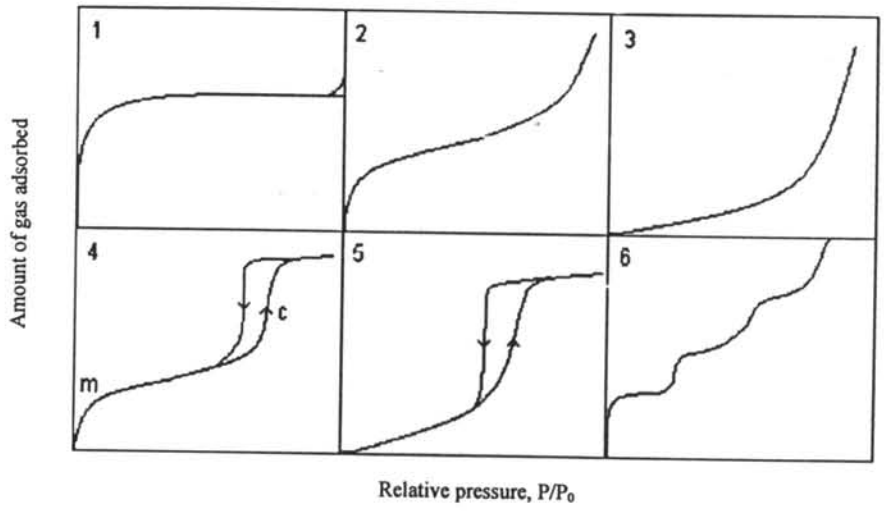

Figure B2 Types of hysteresis loop according to De Boer classification.

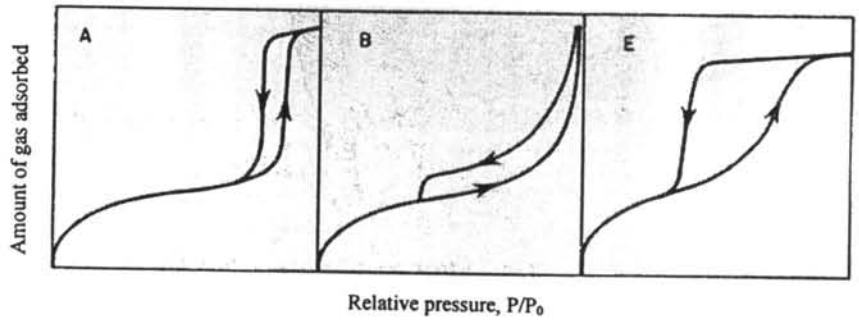

Figure B3 Types of hysteresis loop according to IUPAC classification.

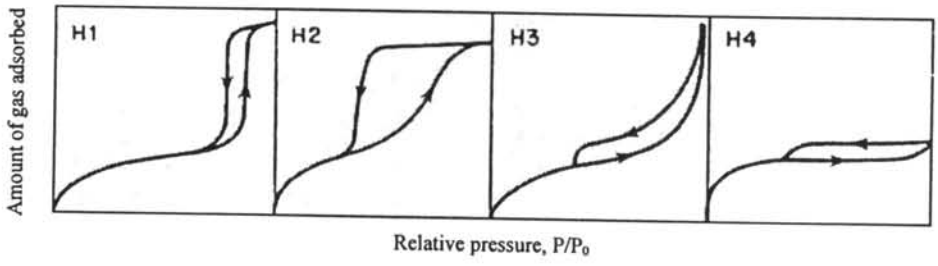

Appendix C Supplementary Results

Figure C1 TEM images of cal-PMH-C_{18}.

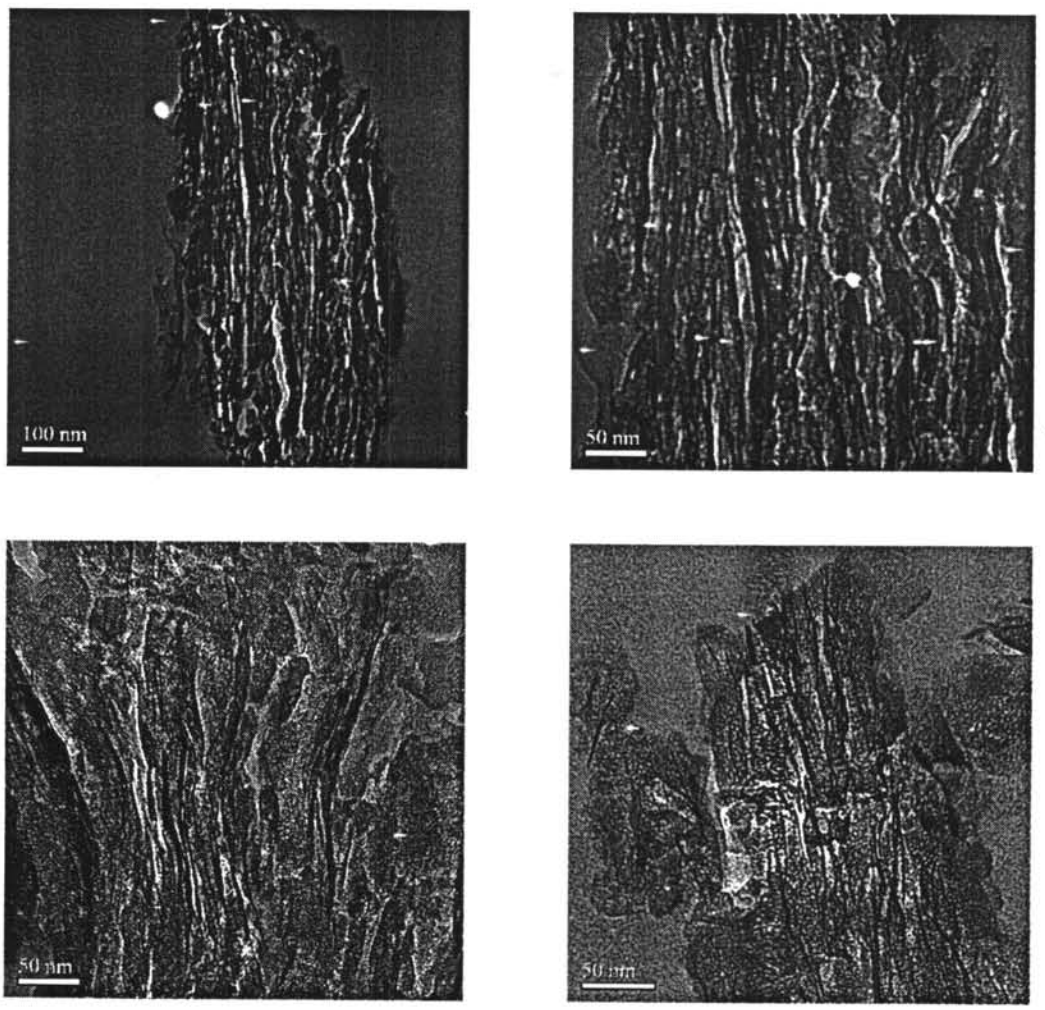

Figure C2 TEM images of cal-PBH-C_{12}.

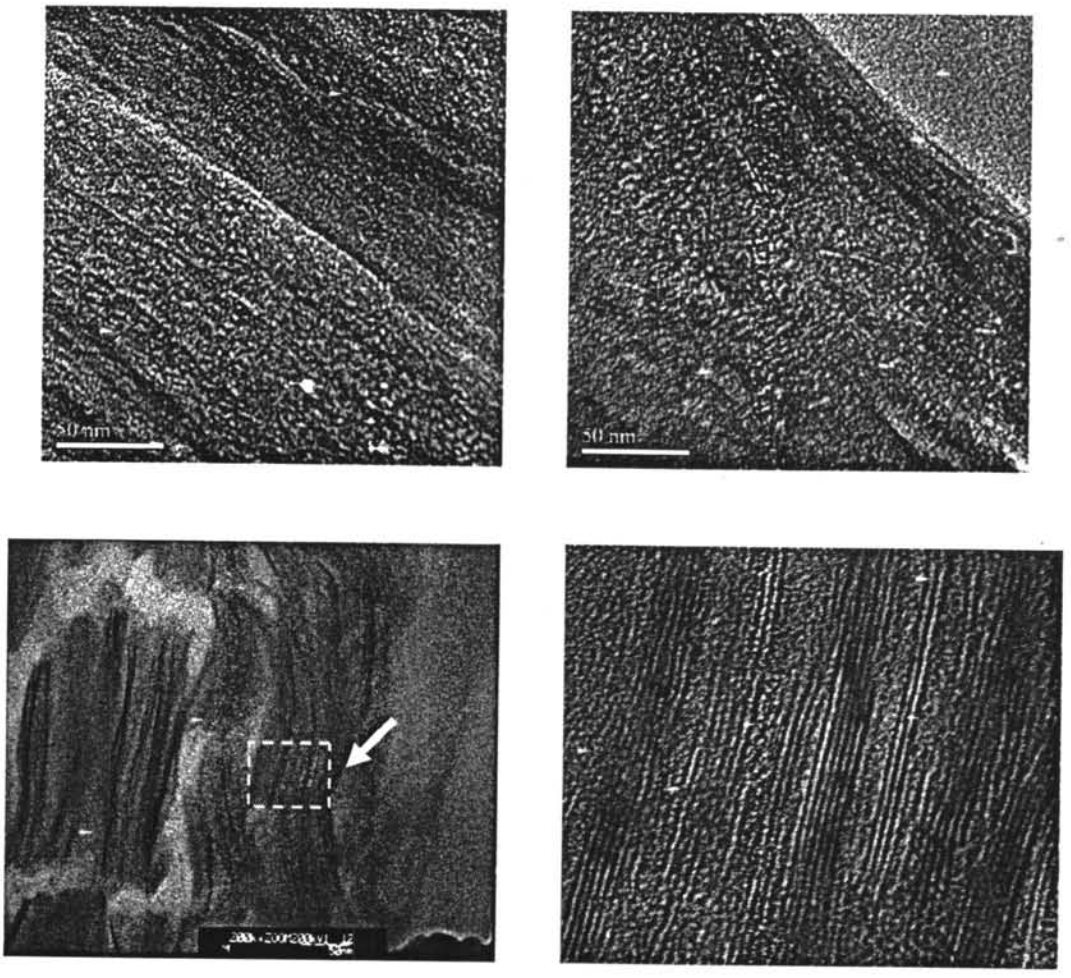

Figure C3 TEM images of cal-PBH-C_{16}.

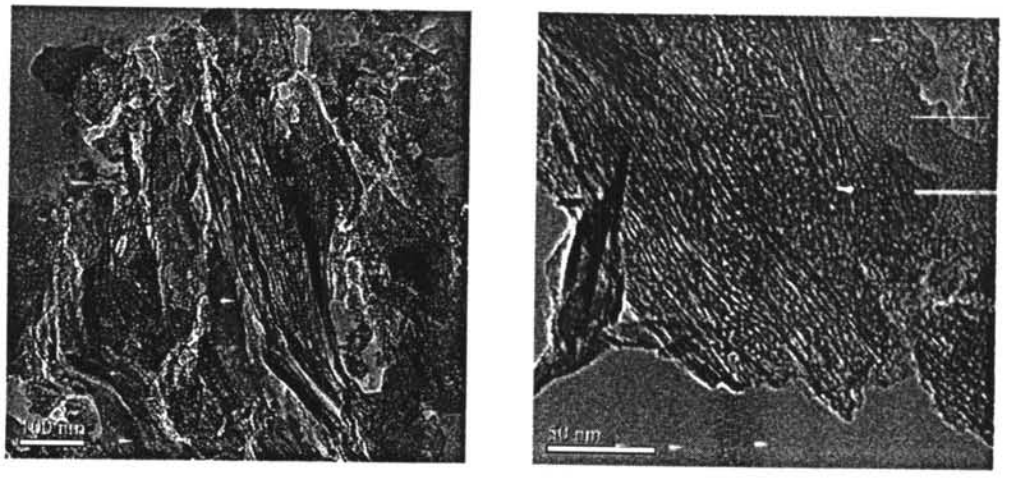

Figure C4 TEM images of cal-PBH-C_{18}.

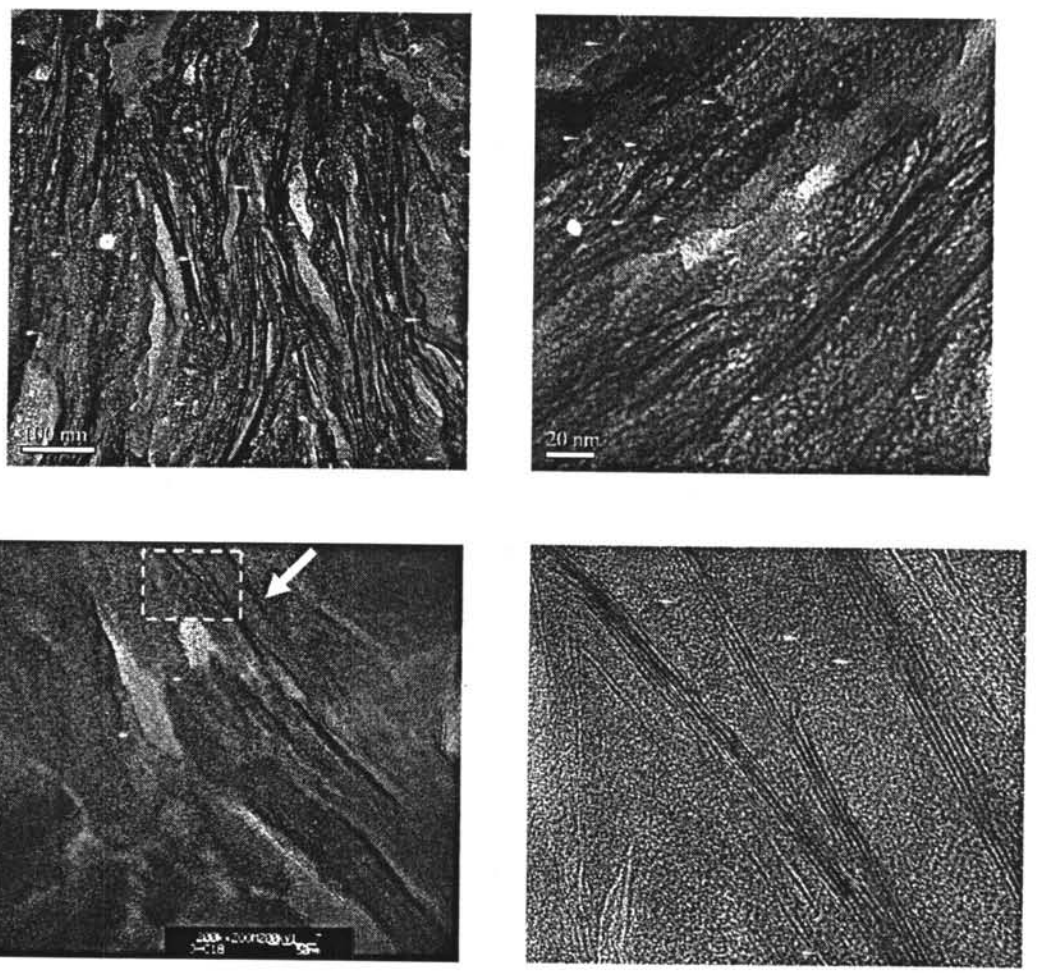

Figure C5 SEM images of nanocomposite film.

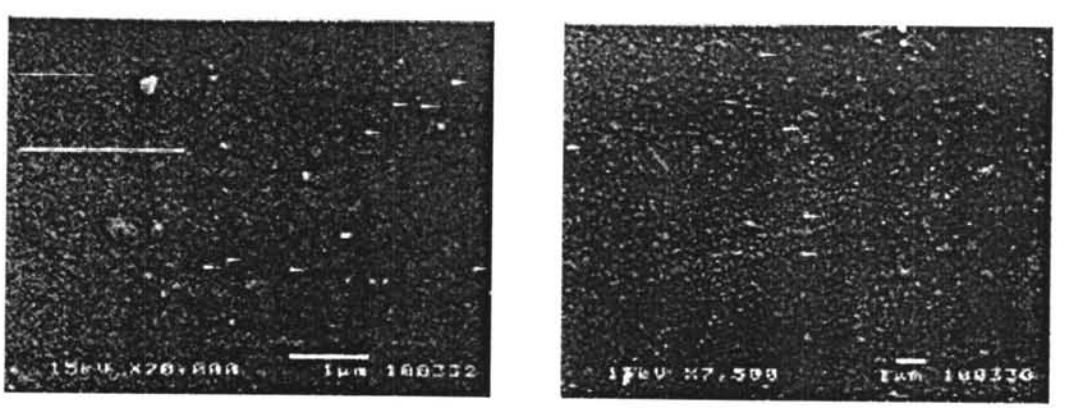

CURRICULUM VITAE

Name: Ms. Sarinya Luangsukrerk

Date of Birth: April 19, 1982

Nationality: Thai

University Education:

2000-2004 Bachelor Degree of Science in Chemistry, Faculty of Science, Cholalongkorn University, Bangkok, Thailand

Working Experience:

2003 Position: Student trainee

Company name: Pollution Control Department